SIRT-1 connects autophagy and release of virus-containing vesicles during picornavirus infection

Alagie Jassey, James Logue, Stuart Weston, Michael A. Wagner, Ganna Galitska, Katelyn Miller, Matthew B. Frieman, and William T. Jackson*

1. Department of Microbiology and Immunology, University of Maryland School of Medicine, 685 W. Baltimore Avenue, Baltimore, MD 21201, USA

*Corresponding Author and Lead Contact: Email: wjackson@som.umaryland.edu

ABSTRACT

Enterovirus D68 is a re-emerging enterovirus which causes acute respiratory illness in infants. EV-D68 infection has recently been associated with Acute Flaccid Myelitis, a severe polio-like neurological disease that causes limb weakness and loss of muscle tone in infants. There is currently no FDA-approved drug or prophylactic vaccine against EV-D68. Here, we investigated the role of the histone deacetylase, SIRT-1, in autophagy and EV-D68 infection. We show that SIRT-1 plays an important role in both autophagy and EV-D68 infection. siRNA-mediated knockdown of the cellular protein blocks basal and stress-induced autophagy and reduces EV-D68 extracellular viral titers. The proviral activity of SIRT-1 does not require deacetylase activity, since transient expression of both wild-type and deacetylase-inactive SIRT-1 mutant plasmids increased EV-D68 release. In non-lytic conditions, EV-D68 is primarily released in extracellular vesicles, and SIRT-1 is required for this process. Knockdown of SIRT-1 further impedes EV-D68 release in the autophagy-deficient ATG-7 knockout cells. Knockdown of SIRT-1 also decreases titers of poliovirus (PV) and SARS-CoV-2, but not Coxsackievirus-B3 (CVB3). CVB3 is the only tested virus that fails to induce SIRT-1 translocation to the cytosol. Our data suggest a correlation between SIRT-1 translocation during viral infection and extracellular vesicle-mediated non-lytic release of infectious viral particles.

SIGNIFICANCE

Picornaviruses, including EV-D68, constitute a significant cause of human disease. EV-D68 infection generally causes mild respiratory tract infection in infants but has

recently been implicated in a severe polio-like neurological disease, AFM. Given the lack of prophylactic vaccines or antivirals against EV-D68, identifying host factors that modulate EV-D68 infection is crucial. Here, we show that SIRT-1 regulates autophagy and EV-D68 infection. Knockdown of SIRT-1 blocked autophagy and impeded the non-lytic release of EV-D68 in extracellular vesicles. We also show that SIRT-1 modulates the release of SARS-CoV-2 and poliovirus but not Coxsackievirus-B3 virus. Our data suggest that many RNA viruses require SIRT-1 for egress and that targeting SIRT-1 could constitute a broad-spectrum antiviral strategy.

INTRODUCTION

Enterovirus D-68 (EV-D68) is a re-emerging enterovirus and a cause of acute respiratory illness in infants. EV-D68 infection has recently been associated with Acute Flaccid Myelitis, a severe polio-like neurological disease that causes limb weakness and loss of muscle tone in infants (1) (2). There is currently no FDA-approved drug or prophylactic vaccine against EV-D68. Hence, it is of utmost importance to study how EV-D68 hijacks host processes to facilitate its life cycle.

EV-D68 is a positive-sense single-stranded RNA virus belonging to the *Piconarviridae* family of enteroviruses. The viral genome encodes a single polyprotein that is immediately processed upon translation by viral proteases into multiple intermediate and mature structural and seven non-structural proteins (3). Picornavirus infection induces extensive rearrangement of cytosolic membranes, beginning with the formation of complex single convoluted membranes, also known as replication vesicles, on the

cytosolic face of which viral RNA replication occurs. These intricate structures eventually morph into double-membrane autophagosome-like structures as the infection progresses (4). Picornavirus replication, maturation, and nonlytic release are known to require autophagy (5–7).

Autophagy is a highly regulated catabolic process that maintains cell survival by targeting superfluous cytoplasmic contents and infectious microorganisms, including pathogenic bacteria and viruses, for degradation. Despite its antimicrobial mechanism, several RNA viruses, including EV-D68, are known to subvert autophagy for their own benefit (8). Autophagy begins with the formation of a phagophore/isolation membrane, which expands and closes to form the autophagosome. The autophagosomes then fuse with endosomes, forming amphisomes, before finally fusing with lysosomes for degradation (9). The conversion of soluble LC3-I to the membrane-associated LC3II, and the degradation of the autophagy receptor, p62, are used as markers for autophagy initiation and completion (autophagic flux) (10). While the mechanistic target of rapamycin complex 1 (MTORC1) and AMP kinase (AMPK) are well-known upstream autophagy regulators by inhibiting or inducing the cellular process, a growing body of evidence recently implicates sirtuin 1 (SIRT-1) as an essential regulator of autophagy downstream of the nucleation complex (11–13).

SIRT-1 belongs to the NAD^+-dependent family of histone deacetylase enzymes, which are known to control several physiological processes. The sirtuin family of enzymes contains seven members (SIRT-1 to 7), which display varying subcellular localization,

with SIRT-1 being the most studied owing to its role in lifespan expansion (14) (15). SIRT-1 has been shown to regulate cellular responses to various stresses, including the cell cycle, apoptosis, inflammation, and more (14). In 2008, SIRT-1, which is typically localized to the nucleus in cancer cells, was demonstrated to form a molecular complex with ATG-5, ATG-7, and LC3 and deacetylates these autophagy-related proteins, thereby regulating autophagy induction (13, 16). In agreement with the above study, SIRT-1 was recently shown to be indispensable for starvation-induced autophagy. The authors demonstrated that during acute amino acid starvation, SIRT-1 deacetylates nuclear LC3, allowing it to interact with TP53INP2. The LC3-TP53INP2 complex then translocates to the cytosol, where LC3 interacts with ATG-7 to initiate autophagosome formation (12). These studies underscore the significance of SIRT-1 for autophagy initiation, but whether SIRT-1 is essential for the later stages of autophagy (autophagic flux) or translocates to the cytosol during starvation or other stress stimuli, such as viral infection, is unknown. SIRT-1 has also been shown to promote the Middle East respiratory syndrome coronavirus infection, but whether SIRT-1 regulates picornavirus infection is unknown (17).

Here, we report that EV-D68 infection induces SIRT-1 translocation to the cytosol. We also show that SIRT knockdown impedes the extracellular vesicle-mediated release of infectious EV-D68 particles. We further demonstrate that the pro-EV-D68 activity of SIRT-1 does not require SIRT-1 deacetylase function and is not dependent on functional autophagy. Moreover, SIRT-1 knockdown reduces extracellular titers of poliovirus (PV) and SARS-CoV-2 but not Coxsackievirus B3 (CVB3). Our results indicate that certain

picornaviruses induce SIRT-1 translocation to the cytosol and require the cellular protein for efficient release.

RESULTS

SIRT-1 is required for autophagy and EV-D68 infection

SIRT-1 has previously been reported to regulate autophagy initiation, but whether the cellular protein is necessary for autophagic flux is unclear (12, 13). We first examined the effect of SIRT-1 knockdown on basal and starvation-induced autophagy. SIRT-1 and scramble knockdown H1HeLa cells were starved or treated with Carbonyl cyanide m-chlorophenylhydrazone (CCCP) to induce or block autophagy, respectively. As shown in Fig. 1A, starvation reduces p62 expression, and CCCP treatment increased LC3 lipidation in the scramble control group as expected. In contrast, acute amino acid starvation did not significantly alter p62 expression, and CCCP treatment failed to trigger LC3II accumulation in SIRT-1 knockdown cells, suggesting that SIRT-1 is essential for basal and starvation-induced autophagy. To further confirm SIRT-1's importance for basal autophagy, we knocked down SIRT-1 and performed immunofluorescence analysis (IFA) against endogenous LC3.

In contrast to the scramble control, which mainly displayed diffused nuclear-localized LC3, SIRT-1 knockdown induced endogenous LC3 puncta accumulation (Fig. 1B). Similar results were observed in GFP-LC3-overexpressing SIRT-1 knockdown cells, wherein knockdown of SIRT triggered GFP-LC3 punta accumulation (Fig. 1C). Together, these results suggest that SIRT-1 is essential for stress-induced and basal autophagy.

SIRT-1 has been shown to be proviral in some cases, but its role in EV-D68 infection is unknown ((17). Given the significance of autophagy for the EV-D68 life cycle, we interrogated the effects of SIRT-1 knockdown on EV-D68 titers. SIRT-1 knockdown reduced both the intracellular (Fig. 1D) and extracellular (Fig. 1E) EV-D68 titers, with the knockdown being more effective in decreasing the extracellular titers than the cell-associated viral titers. Next, we assessed the effect of SIRT-1 overexpression on EV-D68 titers. Both wild-type (SIRT-1 WT) and the deacetylase inactive mutant (SIRT-1 H363Y) increased EV-D68 extracellular titers (Fig. 1F).

SIRT-1 knockdown reduces the extracellular vesicle-mediated release of infectious EV-D68 viral particles

Since SIRT-1 knockdown reduces the extracellular EV-D68 titer an order of magnitude more than the intracellular titers, we posit that SIRT-1 proviral activity promotes non-lytic viral release. Hepatitis A Virus, a member of the *Piconarviridae* family, has been previously reported to be released in exosomes. Hence, we asked whether EV-D68 is similarly released in extracellular vesicles (EVs) and whether SIRT-1 is essential for this process. We knocked down SIRT-1 and isolated EVs for viral titer measurement. As shown in Fig. 2A, EV-D68 appears to be released chiefly in EVs compared to the post-spin supernatant (PSS), and SIRT-1 knockdown severely impeded the extracellular vesicle-mediated release of EV-D68. We knocked down SIRT-1 to understand its impact on viral release. We also examined the expression of CD63, the most widely used marker for exosomes/multivesicular bodies by western blot. As depicted in Fig. 2B, SIRT-1 knockdown increased CD63 expression compared to the scramble control.

Given the increase in CD63 expression in SIRT-1 knockdown cells, we hypothesize that knockdown of SIRT-1 may prevent the exocytosis of CD63-positive EVs. To confirm this hypothesis, we infected SIRT-1 knockdown cells for 4 h and isolated the EVs for western blotting against CD63. As shown in Fig. 2C, SIRT-1 knockdown increased CD63 expression in the whole cell lysate. Our IFA analysis in Fig. 2D also showed the aggregation of large CD63-positive punta in SIRT-1 knockdown cells, as previously observed (18). Interestingly, for the extracellular vesicle fraction, we observed that SIRT-1 knockdown decreased the release of CD63 positive EVs during EV-D68 infection compared to the scramble control, suggesting that SIRT-1 is essential for releasing virus-loaded CD63 positive EVs (Fig. 2C). Together, these results indicate that EV-D68 is mostly non-lytically released in EVs and that SIRT-1 is indispensable for this process.

The proviral activity of SIRT-1 does not require functional autophagy

Poliovirus has previously been reported to be non-lytically released in autophagosomes. Given that SIRT-1 regulates autophagy, which, in turn, regulates EV-D68 infection, we asked whether the proviral activity of SIRT-1 depends on functional autophagy. We first examined whether SIRT-1 colocalizes with ATG-7 during EV-D68 infection. As shown in Fig. 3A, EV-D68 induces ATG-7 puncta formation, which colocalizes with SIRT-1. We next knocked down SIRT-1 in ATG-7-KO cells, which are known to be defective in autophagosome formation, followed by EV-D68 infection. Knockdown of SIRT-1 decreased EV-D68 extracellular titers in ATG-7 KO cells without significantly altering the intracellular titers (Fig. 3B), suggesting that the proviral function of SIRT-1 does not

require functional autophagy. We next examined the effect of ATG-7-KO on EV-D68 release. ATG-7 KO severely impeded both extracellular and EV-mediated release of EV-D68 (Fig. 3C), consistent with the importance of autophagy for picornavirus release (5).

EV-D68 infection induces exportin-1 independent SIRT-1 translocation to the cytosol

Given SIRT-1's proviral role in EV-D68 infection, we asked whether EV-D68 infection alters SIRT-1 protein expression or subcellular localization. We infected H1HeLa cells for various time points before subjecting the cells to IFA against SIRT-1. As indicated in Fig. 4A, SIRT-1 is localized to the nucleus in the mock-infected cells. EV-D68 infection, on the other hand, induced translocation of a fraction of SIRT-1 to the cytosol, beginning at 3hpi (Fig. 4A). To understand whether SIRT-1 translocation during EV-D68 infection is dependent on exportin-1, the major mammalian nuclear export protein, we pretreated H1HeLa cells with and without leptomycin-B, a specific exportin-1 inhibitor, followed by EV-D68 infection (19, 20). As shown in Fig. 4D, leptomycin-B treatment did not impede SIRT-1 translocation induced by EV-D68 infection. We then examined the effect of EV-D68 infection on SIRT-1 protein expression. Results in Fig. 4B and its associated densitometry analysis (Fig. 4C) revealed that in contrast to starvation, which marginally decreased SIRT-1 expression, EV-D68 infection does not significantly impact SIRT-1 protein expression.

SIRT-1 is not required for EV-D68 binding, entry, or replication

Because SIRT-1 translocates to the cytosol at approximately the time of peak viral RNA replication (3hpi), we asked whether SIRT-1 is necessary for viral RNA replication. We first examined whether SIRT-1 is translocated to viral RNA replication sites by conducting IFA using antibodies against SIRT-1 and dsRNA, which detects viral RNA replication intermediates (21). Our data show that SIRT-1 does not colocalize with dsRNA (Fig. 5A). In contrast, GBF-1, a host factor important for forming picornavirus replication organelles, colocalized to dsRNA (Fig. 5B) (22, 23). Next, we performed a time-course infection in the scramble and SIRT-1 knockdown cells for qPCR-based viral RNA replication determination. As indicated in Fig. 5C, SIRT-1 knockdown only marginally reduced EV-D68 genome replication. To rule out the effect of SIRT-1 knockdown on early viral entry, we performed binding and entry assays using SIRT-1 knockdown cells. Depleting SIRT-1 did not significantly affect EV-D68 binding (Fig. 5D) or entry (Fig. 5E) compared to the scramble control. These results suggest that SIRT-1's antiviral activity does not involve blocking viral entry or viral RNA replication.

SIRT-1 Reduces PV, not CVB3, titers

We next sought to understand whether SIRT-1 modulates the infection of other medically essential picornaviruses, including PV and CVB3. While protective vaccines are available for PV, few vaccine-derived PV infection cases exist. On the other hand, there is no vaccine or treatment against CVB3, a significant cause of myocarditis and neurological disorders in infants. Therefore, identifying host factors that influence the infection of these viruses could help control their infection. We first examined whether PV and CVB3 alter the subcellular localization of SIRT-1. To our surprise, while PV,

similar to EV-D68, induces SIRT-1 translocation to the cytosol, CVB3 did not (Fig. 6A). We then examined the impact of SIRT-1 knockdown on PV and CVB3 infection. SIRT-1 knockdown marginally reduced PV intracellular titers but significantly decreased its extracellular titers (Fig. 6B and 6C). In contrast, knockdown of SIRT-1 did not alter CVB3 intracellular titers but slightly increased CVB3 extracellular titers (Fig. 6D and 6E). These results indicate that certain but not all picornaviruses require SIRT-1 for their egress from infected cells.

Knockdown of SIRT-1 reduces SARS-CoV-2 titers

SIRT-1 has previously been reported to be essential for Middle Eastern respiratory syndrome (MERS) coronavirus infection (17). Given the current ongoing SARS-CoV-2 pandemic's significance and to identify host factors/processes important for SARS-CoV-2 infection, we asked whether SIRT-1 is necessary for SARS-CoV-2 infection. A549-ACE-2 cells were transfected with either scramble or SIRT-1 siRNA for 48 h (Fig. 7B), followed by SARS-CoV-2 infection for 24 h. As shown in Fig. 7C, the knockdown of SIRT-1 impeded SARS-CoV-2 release. We then examined the impact of SARS-CoV-2 infection on SIRT-1's subcellular localization. As indicated in Fig. 7A, SARS-CoV-2 infection triggers SIRT-1 translocation to the cytosol, similar to PV and EV-D68. These results show that, as with MERS-CoV, SIRT-1 is essential for SARS-CoV-2 infection.

DISCUSSION

Here, we demonstrate that SIRT-1 is essential for basal and starvation-mediated autophagy. Depletion of SIRT-1 blocks basal autophagy and attenuates starvation-induced autophagic degradation. In addition, we show that EV-D68 in pre-lytic conditions is mainly released in EVs and that SIRT-1 is essential for the extracellular vesicle-mediated release of EV-D68. Consequently, the knockdown of SIRT-1 severely decreases infectious EV-D68 particles released in EVs. Knockdown of SIRT-1 also attenuates the release of PV and SARS-CoV-2 but marginally increases CVB3 egress. Our results suggest that some viruses induce SIRT-1 translocation to the cytosol to promote their vesicular release.

Our data show that SIRT-1 plays a cellular role in modulating basal autophagy. Depletion of SIRT-1 increased LC3II accumulation (Fig. 1A) and enhanced endogenous (Fig. 1B) and GFP-LC3 (Fig. 1C) punta formation under basal conditions. These findings highlight the significance of SIRT-1 for basal autophagic degradation and suggest that SIRT-1 may somehow regulate autophagosomal acidification or autophagosome-lysosome fusion. Consistent with the presumption that SIRT-1 regulates autophagosome acidification, Latifkar et al. showed that depleting SIRT-1 impairs lysosomal function by decreasing subunit A of V1 (ATP6V1A), which is one of the subunits of V-ATPases (enzymes responsible for endosomal/lysosomal acidification) (18). SIRT-1 knockdown mimics autophagic flux blockage by bafilomycin, a well-known V-ATPase inhibitor.

Our data also show that SIRT-1 regulates starvation-induced autophagy. The kinetic studies in our supplemental data revealed that starvation induces rapid SIRT-1 translocation to the cytosol as early as 1h post-treatment (Fig. S1A). This finding is consistent with the notion that SIRT-1 drives autophagosome formation during amino acid starvation. Although starvation slightly decreased SIRT-1 protein expression by western blot, pharmacological inhibition of autophagic flux failed to restore SIRT-1 expression. Moreover, SIRT-1 did not colocalize with p62 in starved cells (Fig. S1B), suggesting that the cellular protein is not a substrate for autophagy.

Previous studies have shown that SIRT-1 forms a complex with cytoplasmic autophagy-related proteins, such as ATG7, ATG5, and LC3, upon acute amino acid starvation (13). However, given SIRT1's nuclear localization, exactly how SIRT-1 might form a molecular complex with the abovementioned proteins has been unclear. Our finding that amino acid starvation induces extensive SIRT-1 translocation provides a plausible explanation for how SIRT-1 interacts with these cytosolic proteins.

While picornaviruses are mainly released by cell lysis, a growing body of evidence indicates that these viruses can be released from intact cells without cell lysis, a phenomenon called non-lytic release. For instance, PV has been shown to escape intact cells through AWOL (autophagosome-mediated exit without lysis), in which virus-containing autophagosomes fuse with the plasma membrane to release virions (5, 24). We show that knockout of ATG-7 reduces EV-D68 extracellular/EV titers, which is consistent with the AWOL model (Fig. 3B and C). Hepatitis A virus (HAV), which is

non-lytic, has been reported to exit cells in an enveloped form known as eHAV (25, 26). Similar events, modulated through the autophagic pathway, have been shown for other picornaviruses(27–29). We show here for the first time that EV-D68 can also exit intact cells non-lytically in EVs. This extracellular vesicle-mediated release of EV-D68 virions is, as we show here, dependent upon the autophagy regulator SIRT-1 (Figures 1E, 2A, 3B).

We noticed that EV-D68 infection induces SIRT-1 translocation to the cytosol starting at 3 hpi. Given that RNA replication peaks at 3hpi, we initially thought SIRT-1 might be essential for viral RNA replication. However, during EV-D68 infection, SIRT-1 did not colocalize to dsRNA (Fig.5A) and its knockdown did not significantly impact EV-D68 RNA replication (Fig. 5C) nor viral binding (Fig. 5D) or entry (Fig. 5E). Instead, our findings suggest that the effect of SIRT-1 on virus production can largely be explained by its prominent role in the re-configuring the exocytosis pathway to promote the release of virus-loaded EVs. Knockdown of SIRT-1 led to the accumulation of large CD63 positive puncta in cells (Fig. 2D), suggesting that the turnover or the release of these vesicles is blocked in the absence of SIRT-1. Interestingly, our western blot data shows a marked decrease in CD63-positive EVs in cells with reduced SIRT-1 expression (Fig. 2C). This finding, coupled with the increased CD63 in the whole-cell lysate (Fig. 2B and C), indicates that the reduction of SIRT-1 attenuates the release of virus-loaded CD63-positive EVs.

Although EV-D68 is known to induce autophagy and block the downstream autophagic maturation, how exactly EV-D68 infection causes autophagy and the specific viral protein(s) involved is not entirely understood (30, 31). Our finding that EV-D68 infection induces SIRT-1 translocation starting at 3 hpi, which coincides with the emergence of lipidated LC3, suggests that SIRT-1 may be essential for virus-induced changes in the autophagic pathway. We observed that EV-D68 infection also induces ATG-7 punta formation, which, intriguingly, partially colocalizes to SIRT-1 (Fig. 3A). Hence, SIRT-1 translocation to the cytosol during EV-D68 infection could constitute a mechanism by which EV-D68 induces the generation and rearrangement of autophagic membranes.

SIRT-1 has previously been demonstrated to be important for MERS-CoV infection (17). Here, we demonstrate that the cellular protein is also crucial for SARS-CoV-2 infection. Our data show that, much like in the MERS-CoV study, knockdown of SIRT-1 decreases SARS-CoV-2 release, suggesting that SIRT-1 may be a shared host factor utilized by many Betacoronaviruses.

Our data show that a portion of nuclear SIRT-1 re-localizes to the cytosol upon infection by EVD-68 and PV. (Fig. 4A, 6A). We also observe that SARS-CoV-2 infection causes SIRT-1 translocation to the cytosol (Fig 7A). These viruses require SIRT-1 for normal virus release. It will be interesting to examine whether other Betacoronaviruses alter the subcellular localization of SIRT-1 and whether SIRT-1 is important for their infection.

CVB3, which does not require SIRT-1, does not induce re-localization of the protein (Fig. 6A). This, along with the finding that SIRT-1 is found on virus-induced extracellular vesicles, suggests to us a central role for SIRT-1 in constructing virus-containing vesicles for extracellular release - but only for some viruses. Why at least one picornavirus has evolved a SIRT-1-independent mechanism for release and what the mechanism might be will help understand how to target specific viruses or broad classes of viruses to prevent their release from infected cells. While we believe SIRT-1 is a common regulator of virus release, it is not a universal one, and identifying the homolog, or paralog, protein playing a parallel role in CVB3 release will undoubtedly shed light on the differences between these otherwise similar viruses.

In summary, our data show that SIRT-1 is essential for basal- and stress-induced autophagy and EV-mediated non-lytic release of EV-D68. We also demonstrated that SIRT-1 is crucial for releasing other important public health viruses, including SARS-CoV-2 and PV, indicating that SIRT-1 may be a common host factor regulating multiple viruses' release. Understanding how SIRT-1 regulates viral egress could open avenues for therapeutic intervention against many viruses.

MATERIALS AND METHODS

Cell culture, plasmids, and viruses

H1HeLa cells were purchased from ATCC and cultured in DMEM supplemented with 10% fetal bovine saline, 1x penicillin/streptomycin, and 1x sodium pyruvate. The cells

were incubated at 37°C in a 5% CO_2 incubator. The wild-type (Flag-SIRT1) and mutant (Flag-SIRT1 H363Y) SIRT-1 plasmids were purchased from Addgene and transfected into cells using lipofectamine 2000. The transfection complex was replaced with basal media 6 h post-transfection.

All work with SARS-CoV-2 was performed in a BSL3 laboratory and approved by our Institutional Biosafety Committee (IBC#00005484). Vero E6 cells overexpressing transmembrane serine protease 2 (TMPRSS2) (VeroT) (ATCC CRL 1586) were cultured in DMEM medium (Quality Biological) supplemented with 10% (vol/vol) heat-inactivated FBS (Sigma), 1% (vol/vol) penicillin-streptomycin (Gemini Bio-Products) and 1% (vol/vol) l-glutamine (2 mM final concentration; Gibco). A549 cells overexpressing human angiotensin-converting enzyme 2 (hACE2, A549/hACE2) were generously provided by Dr. Brad Rosenberg (32). They were cultured in DMEM medium (Quality Biological) supplemented with 10% (vol/vol) heat-inactivated FBS (Sigma), and 1% (vol/vol) penicillin-streptomycin (Gemini Bio-Products).

Western blot

Cells were lysed using RIPA buffer supplemented with cOmplete Tablets Mini Protease Inhibitor Cocktail. The lysates were incubated on ice for at least 30 minutes before being clarified at 12000 rpm for 30 minutes. The supernatants were transferred into Eppendorf tubes, and protein concentrations were determined by Bradford assay. Lysates were then cooked and loaded onto SDS-PAGE. Following transfer onto PVDF membranes, the membranes were blocked in 5% skim milk for 1 h, washed twice with TBST, and stained with the following primary antibodies: anti-SQSTM1/p62, anti-LC,

anti-b-actin, at 1: 1000 dilutions, and anti-CD63 (1: 250) overnight. The membranes were stained with the secondary antibodies for 1 h at room temperature and imaged using the Chemidoc machine after two washes.

Immunofluorescence analysis (IFA)

The cells were fixed with 4% paraformaldehyde at room temperature for 20 minutes and then permeabilized with 0.3% Triton-X for 30 minutes. The cells were blocked with 3% BSA for 1 h on a shaker and incubated with primary antibodies at 1: 250 dilutions overnight at 4°C. The cells were subsequently washed twice with PBS, incubated with the secondary antibodies (1:250), rewashed three times, and imaged with the revolve fluorescence microscope.

Extracellular vesicle isolation

Extracellular vesicles were isolated using the Invitrogen Total Exosome Isolation Reagent (from cultured cells). In brief, 1 ml of cell culture supernatants were clarified at 2000 x g for 30 minutes. The supernatants were then transferred to Eppendorf tubes, and 500 µl of the exosome isolation buffer was added and incubated at 4°C overnight. At the end of the incubation, the tubes were centrifuged for 1 h at 10000 x g. The supernatants were transferred to new Eppendorf tubes, and the pellets were resuspended in PBS for western blot or plaque assay.

RNA isolation and qPCR

TRIzol was used to isolate total RNA according to the manufacturer's instructions, and cDNA was synthesized using the Thermo Scientific RevertAid H Minus First Strand cDNA Synthesis Kit. KiCqStart SYBR qPCR Ready Mix was used to perform qPCR using the Fast Dx Real-Time PCR Instrument (Applied Biosystems). Primers specific to the 5′ untranslated region (5′ TAACCCGTGTGTAGCTTGG-3′ and 5′ -ATTAGCCGCATTCAGGGGC-3′) were used to amplify EV-D68, and gene expression was normalized to GAPDH and plotted as relative expression compared to the 0h infection-only time point.

Plaque assay

The cells were washed twice with PBS for cell-associated titer determination and scraped in 1ml PBS, after which they were subjected to three free-thaw cycles and added to H1HeLa cells for 30 minutes. Cells were then overlaid with a 1:1 ratio of 2x MEM and 2% agar for 48 h before staining plaques with crystal violet. For extracellular titers, 1 ml of supernatants were collected and treated as the cell-associated titer without being subjected to free-thaw cycles.

siRNA transfections

siRNAs were transfected into cells using lipofectamine as previously described. In brief, 200 nM of siRNA and 10 µl of Lipofectamine 2000 were separately incubated in Opti-MEM at room temperature for 5 minutes. The siRNAs and lipofectamine were mixed and incubated for 20 minutes before being added to cells that were 40% confluent. The transfection complexes were replaced with growth media at 6 h

post-transfection. The cells were then used for viral infection or western blot for transfection efficiency determination.

Virus entry assays

Scramble and SIRT-1 knockdown cells were pre chilled on ice for 30 minutes for viral binding assay. The cells were then infected with EV-D68 (MOI =30) for 1 h on ice. The inoculum was removed, and the cells were washed twice with PBS, scraped, freeze-thawed 3 times, and stored at -80°C for plaque assay.

For viral entry, scramble and SIRT-1 knockdown cells were similarly pre chilled on ice for 30 minutes and then infected with EV-D68 for 30 minutes on ice. The unbound viral particles were washed off with PBS before shifting the cells to 37°C, allowing viral entry for 1 h. The cells were finally washed with PBS, scraped into Eppendorf tubes, and prepared for plaque assay.

SARS-CoV-2 titer determination by plaque assay

Plaque assays were performed as described previously (33). Briefly, 12-well plates were seeded with 2 x 10^5 VeroT cells/well one day before processing. On the day of processing, media was removed from the 12-well plates, and 200 µl of dilutions of virus stock or collected cell supernatants in DMEM were added to each well. Plates were incubated at 37°C (5% CO^2) for 1 hour with rocking every 15 minutes. Following incubation, 2 ml of plaque assay media, DMEM containing 0.1% agarose (UltraPure™) and 2% FBS (Gibco), was added to each well and incubated for 48 h at 37°C (5% CO^2). Following incubation, plates were fixed with 4% paraformaldehyde, stained with 0.25%

crystal violet (w/v), plaques counted, and titers calculated as plaque-forming units (PFU)/ml.

siRNA Knockdown Protocol for SARS-CoV-2 infection

siRNA knockdown assays were performed as described previously (34). Briefly, A549/hACE2 cells were seeded in 24-well cell culture plates one day before siRNA treatment. On the day of treatment, 4.4 µl Opti-MEM (Gibco) and 2.2 µl Oligofectamine (Thermo Scientific) were combined and incubated for 5 minutes at room temperature. This mixture was then added to 35.5 µl Opti-MEM and 0.8µl of 50 µM siRNA and incubated for 20 minutes at room temperature. Following incubation, a further 177 µl of Opti-MEM was added to the transfection mixture, media were removed from cells, and 200 µl of transfection mixture was added. After a 4 h incubation at 37°C/5% CO^2, 200 µl of DMEM (+20% FBS) was added to the cells resulting in a final concentration of 10% FBS. Cells were then incubated at 37°C/5% CO^2 overnight. Following incubation, cells were infected with SARS-CoV-2 (WA1, MOI = 0.01 for titer, MOI = 0.5 for IFA), and supernatants were collected 24 hours post-infection. SARS-CoV-2 titers from supernatants were determined by plaque assay.

Statistical analysis

GraphPad Prism software (Version 7.03) was used for all statistical analyses, and values represent the mean ± standard error of the mean (SEM) of at least 3 independent repeats. Student t-test for comparison and a p-value of < 0.05. was considered statistically significant.

ACKNOWLEDGEMENTS

We thank Sohha Ariannejad for assistance and the members of the Jackson, Frieman, and Coughlan labs for thoughtful discussion. This work was funded by NIH/NIAID grants R01141359, R01104928 to W.T.J. and R21158134 to W.T.J. and M.B.F.

FIGURE LEGENDS

Figure 1. SIRT-1 is required for autophagy, and its KD reduces EV-D68 titers: (A) H1HeLa cells were transfected with scrambled or SIRT-1 siRNA for 48 h. The cells were subsequently starved or treated with CCCP (10 μM) for 4 h. Lysates were harvested and analyzed by western blot. (B) Cells were transfected with the indicated siRNAs for 48 h before being fixed and subjected to IFA against endogenous LC3. (C) H1HeLa cells were transfected with either scramble or SIRT-1 siRNA for 48 h. GFP-LC3 transfection was initiated at 24 h post siRNA transfected for 24 h. The cells were then fixed, and images were acquired with a revolve microscope. (D and E) H1HeLa cells were transfected with either scramble control or SIRT-1 siRNAs for 48 h. The cells were then infected with EV-D68 (MOI = 0.1) for 5 h. The intracellular (D) and extracellular (E) particles were collected for plaque assay. (F) Cells were transfected with the indicated plasmids for 24 h, before being infected with EV-D68 (MOI = 0.1) for 5 h. The extracellular particles were collected and analyzed by a plaque assay. (* = $p < 0.05$; ** = $p < 0.01$; ns = not significant.). Error bars denote the mean ± SEM of 3 independent repeats. Unpaired student's t-test was used for the statistical analyzes (**= $p< 0.01$;* = $p \leq 0.05$; ns=not significant.) Scale bar = 6 μm.

Figure 2. SIRT-1 KD reduces extracellular vesicle-mediated EV-D68 release

H1HeLa cells were transfected with SIRT-1 and Scramble siRNAs for 48 h. (A) The cells were infected with EV-D68 (MOI = 0.1) for 5 h, and EVs were isolated for viral titer measurement by plaque assay. (B) Cells were transfected as in A, and the whole-cell lysates (WCL) were collected and prepared for western blot against CD63. (C) H1HeLa cells were transfected with the indicated siRNAs for 48 h. The cells were either left uninfected or infected with MOI 30 of EV-D68 for 4 h. The EVs and WCL were prepared for western blot against the indicated proteins. (D) Cells were plated on cover slides and transfected with scramble or SIRT-1 siRNA for 48 h. The cells were then fixed and subjected to immunofluorescence analysis against CD63. Arrows indicate large CD63 puncta. Error bars indicate mean ± SEM. Unpaired student's t-test was used for the statistical analyzes (**= $p < 0.01$;* = $p \leq 0.05$.) Scale bar = 6.5 μm.

Figure 3. The proviral activity of SIRT-1 does not require functional autophagy

(A) H1Hela cells were infected with EV-D68 (MOI =30) for 4 h. The cells were fixed and immuno-stained with antibodies against SIRT-1 and ATG-7. (B) H1HeLa and ATG-7 KO cells were infected with 0.1 MOI of EV-D68 for 5h, followed by a plaque assay-based viral titer measurement. (C) Cells were infected as in B. The extracellular vesicles were isolated as described in the materials and methods and viral titers were determined by a plaque assay.

Figure 4. EV-D68 infection induces SIRT-1 translocation to the cytosol. (A) Cells were infected for the indicated time points, and IFA was performed against SIRT-1. Nuclei were demarcated with dapi. (B) H1HeLa cells were infected for 4 h. Lysates were collected for western blot against SIRT-1. (C) Densitometry quantitation of B. (D) Cells were pretreated with 50 nM of LMB for 2 h. The cells were then infected for 30 minutes (adsorption) and incubated with and without LMB until the end of the infection (4h) for IFA against SIRT-1. For all experiments, n = 3 independent repeats. MOI = 30 for all experiments. Scale bar = 6.2 μm.

Figure 5. SIRT-1 is not required for EV-D68 entry and replication. (A) Cells were infected for the indicated time point, fixed, and processed for IFA against SIRT-1 and dsRNA. (B) Cells were infected as in A for IFA against GBF-1, and dsRNA (C) H1HeLa cells were transfected with scramble or SIRT-1 siRNA for 48 h. The cells were then infected (MOI = 0.1) for the indicated time point for the qPCR assay. (D and E) Cells were transfected as in B, and virus binding and entry assays were performed as described in the materials and methods. (ns = non significant)
Scale bar = 6.2 μm.

Figure 6. SIRT-1 KD reduces PV, not CVB3 titers. (A) H1HeLa cells were mock-infected or infected with PV or CVB 3 for 4 h. The cells were fixed, and IFA was done against SIRT-1 MOI = 30. (B and C) Cells were transfected with scramble or SIRT-1 siRNAs for 48 h before being infected (MOI = 0.1) for 5 h. Viral titers were determined by a plaque assay. (D and E) Cells were transfected and infected with CVB3

as in B. n = 3 independent experiments, and error bars represent mean ± SEM. (*** = $p < 0.001$; * = $p \leq 0.05$; ns = not significant.). Scale bar = 7.5 μm.

Figure 7. SARS-CoV-2 infection causes SIRT- translocation to the cytosol. (A) A549-ACE2 cells were infected with SAR-CoV-2 (MOI =0.5) for 24 h. The cells were fixed and subjected to IFA against SIRT-1 and SARS-CoV-2 nucleoprotein. (B) A549-ACE2 cells were transfected with SIRT-1 siRNA for 48 h. Lysates were analyzed by western blot. (C) Cells were transfected as in B and infected (MOI 0.01) for 48 h before being subjected to a plaque assay for viral titer measurement. (** = $p < 0.01$). Scale bar = 30 μm.

Supplemental Figure 1. SIRT-1 does not colocalize with p62. (A) H1HeLa cells were starved for the indicated periods, fixed, and subjected to IFA against SIRT-1. (B) H1HeLa cells were treated with and without the Axe starvation media for 2 h. The cells were then fixed and immunostained using antibodies against SIRT-1 and p62.

REFERENCES

1. Lang M, Mirand A, Savy N, Henquell C, Maridet S, Perignon R, Labbe A, Peigue-Lafeuille H. 2014. Acute flaccid paralysis following enterovirus D68 associated pneumonia, France, 2014. Euro Surveill 19.

2. Eshaghi A, Duvvuri VR, Isabel S, Banh P, Li A, Peci A, Patel SN, Gubbay JB. 2017. Global Distribution and Evolutionary History of Enterovirus D68, with Emphasis on the 2014 Outbreak in Ontario, Canada. Front Microbiol 8:257.

3. Esposito S, Bosis S, Niesters H, Principi N. 2015. Enterovirus D68 Infection. Viruses 7:6043–6050.

4. Belov GA, Nair V, Hansen BT, Hoyt FH, Fischer ER, Ehrenfeld E. 2012. Complex dynamic development of poliovirus membranous replication complexes. J Virol 86:302–312.

5. Jackson WT, Giddings TH Jr, Taylor MP, Mulinyawe S, Rabinovitch M, Kopito RR, Kirkegaard K. 2005. Subversion of cellular autophagosomal machinery by RNA viruses. PLoS Biol 3:e156.

6. Jackson WT. 2014. Poliovirus-induced changes in cellular membranes throughout infection. Curr Opin Virol 9:67–73.

7. Shi J, Luo H. 2012. Interplay between the cellular autophagy machinery and positive-stranded RNA viruses. Acta Biochim Biophys Sin 44:375–384.

8. Ahmad L, Mostowy S, Sancho-Shimizu V. 2018. Autophagy-Virus Interplay: From

Cell Biology to Human Disease. Front Cell Dev Biol 6:155.

9. Mannack, Lane. 2015. The autophagosome: current understanding of formation and maturation. Res Rep Biochem.

10. Corkery D, Wu Y-W, Dowaidar M. 2021. Guidelines for the use and interpretation of assays for monitoring autophagy. Autophagy.

11. Green DR, Levine B. 2014. To Be or Not to Be? How Selective Autophagy and Cell Death Govern Cell Fate. Cell 157:65–75.

12. Huang R, Xu Y, Wan W, Shou X, Qian J, You Z, Liu B, Chang C, Zhou T, Lippincott-Schwartz J, Liu W. 2015. Deacetylation of nuclear LC3 drives autophagy initiation under starvation. Mol Cell 57:456–466.

13. Lee IH, Cao L, Mostoslavsky R, Lombard DB, Liu J, Bruns NE, Tsokos M, Alt FW, Finkel T. 2008. A role for the NAD-dependent deacetylase Sirt1 in the regulation of autophagy. Proc Natl Acad Sci U S A 105:3374–3379.

14. Chalkiadaki A, Guarente L. 2015. The multifaceted functions of sirtuins in cancer. Nat Rev Cancer 15:608–624.

15. Jing H, Lin H. 2015. Sirtuins in epigenetic regulation. Chem Rev 115:2350–2375.

16. Bai W, Zhang X. 2016. Nucleus or cytoplasm? The mysterious case of SIRT1's subcellular localization. Cell Cycle. Taylor & Francis.

17. Weston S, Matthews KL, Lent R, Vlk A, Haupt R, Kingsbury T, Frieman MB. 2019. A Yeast Suppressor Screen Used To Identify Mammalian SIRT1 as a Proviral Factor

for Middle East Respiratory Syndrome Coronavirus Replication. J Virol 93.

18. Latifkar A, Ling L, Hingorani A, Johansen E, Clement A, Zhang X, Hartman J, Fischbach C, Lin H, Cerione RA, Antonyak MA. 2019. Loss of Sirtuin 1 Alters the Secretome of Breast Cancer Cells by Impairing Lysosomal Integrity. Dev Cell 49:393–408.e7.

19. Fornerod M, Ohno M, Yoshida M, Mattaj IW. 1997. CRM1 is an export receptor for leucine-rich nuclear export signals. Cell 90:1051–1060.

20. Fukuda M, Asano S, Nakamura T, Adachi M, Yoshida M, Yanagida M, Nishida E. 1997. CRM1 is responsible for intracellular transport mediated by the nuclear export signal. Nature 390:308–311.

21. Weber F, Wagner V, Rasmussen SB, Hartmann R, Paludan SR. 2006. Double-stranded RNA is produced by positive-strand RNA viruses and DNA viruses but not in detectable amounts by negative-strand RNA viruses. J Virol 80:5059–5064.

22. Richards AL, Soares-Martins JAP, Riddell GT, Jackson WT. 2014. Generation of Unique Poliovirus RNA Replication Organelles. mBio https://doi.org/10.1128/mbio.00833-13.

23. Belov GA, Altan-Bonnet N, Kovtunovych G, Jackson CL, Lippincott-Schwartz J, Ehrenfeld E. 2007. Hijacking components of the cellular secretory pathway for replication of poliovirus RNA. J Virol 81:558–567.

24. Richards AL, Jackson WT. 2012. Intracellular vesicle acidification promotes

maturation of infectious poliovirus particles. PLoS Pathog 8:e1003046.

25. Feng Z, Hensley L, McKnight KL, Hu F, Madden V, Ping L, Jeong S-H, Walker C, Lanford RE, Lemon SM. 2013. A pathogenic picornavirus acquires an envelope by hijacking cellular membranes. Nature 496:367–371.

26. Rivera-Serrano EE, González-López O, Das A, Lemon SM. 2019. Cellular entry and uncoating of naked and quasi-enveloped human hepatoviruses. Elife 8.

27. Robinson SM, Tsueng G, Sin J, Mangale V, Rahawi S, McIntyre LL, Williams W, Kha N, Cruz C, Hancock BM, Nguyen DP, Sayen MR, Hilton BJ, Doran KS, Segall AM, Wolkowicz R, Cornell CT, Whitton JL, Gottlieb RA, Feuer R. 2014. Coxsackievirus B exits the host cell in shed microvesicles displaying autophagosomal markers. PLoS Pathog 10:e1004045.

28. Chen Y-H, Du W, Hagemeijer MC, Takvorian PM, Pau C, Cali A, Brantner CA, Stempinski ES, Connelly PS, Ma H-C, Jiang P, Wimmer E, Altan-Bonnet G, Altan-Bonnet N. 2015. Phosphatidylserine vesicles enable efficient en bloc transmission of enteroviruses. Cell 160:619–630.

29. Sin J, McIntyre L, Stotland A, Feuer R, Gottlieb RA. 2017. Coxsackievirus B escapes the infected cell in ejected mitophagosomes. J Virol 91.

30. Corona AK, Saulsbery HM, Corona Velazquez AF, Jackson WT. 2018. Enteroviruses Remodel Autophagic Trafficking through Regulation of Host SNARE Proteins to Promote Virus Replication and Cell Exit. Cell Rep 22:3304–3314.

31. Jassey A, Wagner MA, Galitska G, Paudel B, Miller K, Jackson WT. 2022.

Starvation after infection restricts enterovirus D68 replication. Autophagy 1–14.

32. Daniloski Z, Jordan TX, Wessels H-H, Hoagland DA, Kasela S, Legut M, Maniatis S, Mimitou EP, Lu L, Geller E, Danziger O, Rosenberg BR, Phatnani H, Smibert P, Lappalainen T, tenOever BR, Sanjana NE. 2021. Identification of Required Host Factors for SARS-CoV-2 Infection in Human Cells. Cell 184:92–105.e16.

33. Coleman CM, Frieman MB. 2015. Growth and Quantification of MERS-CoV Infection. Curr Protoc Microbiol 37:15E.2.1–9.

34. Weston S, Baracco L, Keller C, Matthews K, McGrath ME, Logue J, Liang J, Dyall J, Holbrook MR, Hensley LE, Jahrling PB, Yu W, MacKerell AD Jr, Frieman MB. 2020. The SKI complex is a broad-spectrum, host-directed antiviral drug target for coronaviruses, influenza, and filoviruses. Proc Natl Acad Sci U S A 117:30687–30698.

Fig. 1 SIRT-1 is required for autophagy and its KD reduced EV-D68 titers

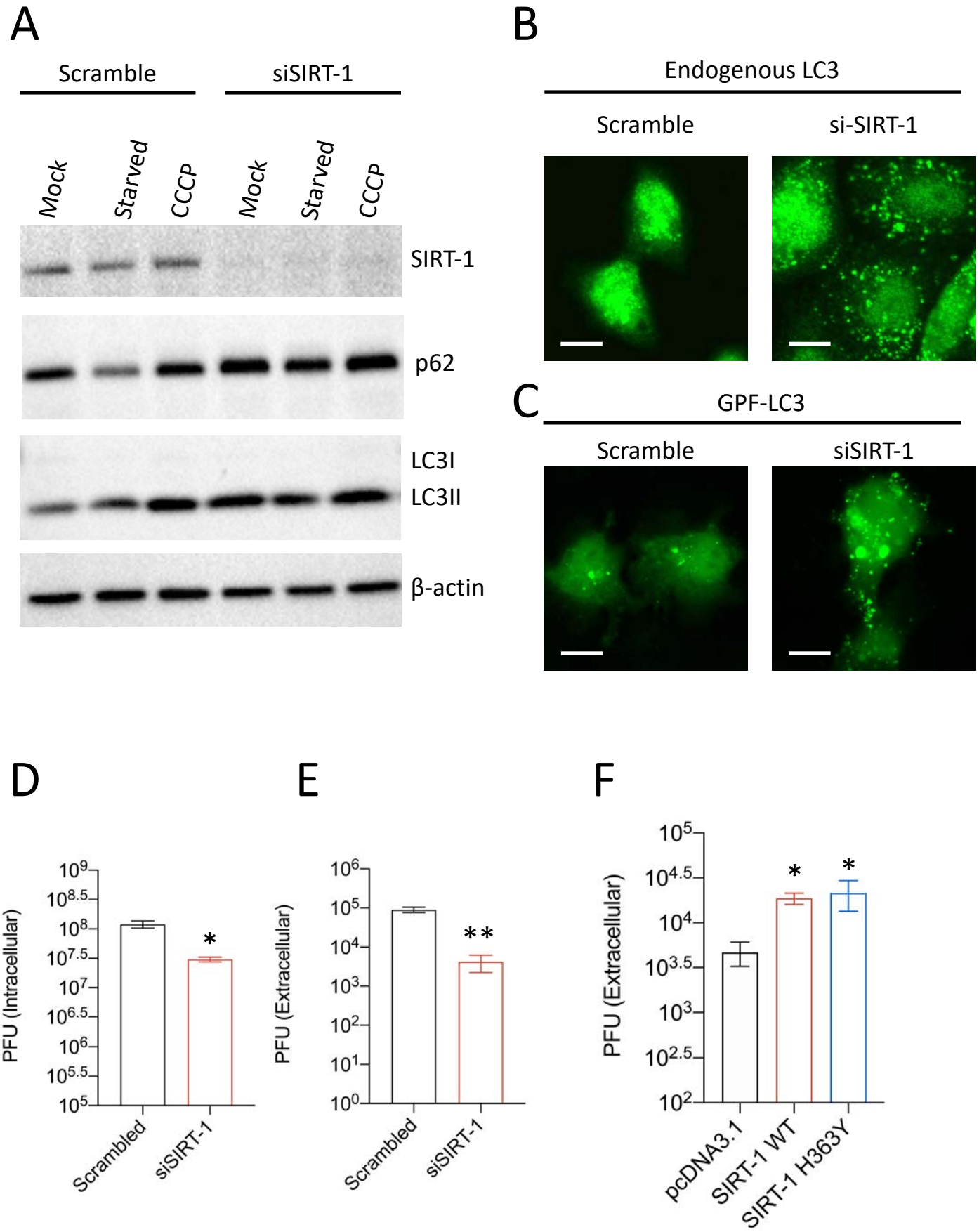

Fig. 2 SIRT-1 KD reduces Extracellular vesicle-mediated release of infectious EV-D68 viral particles

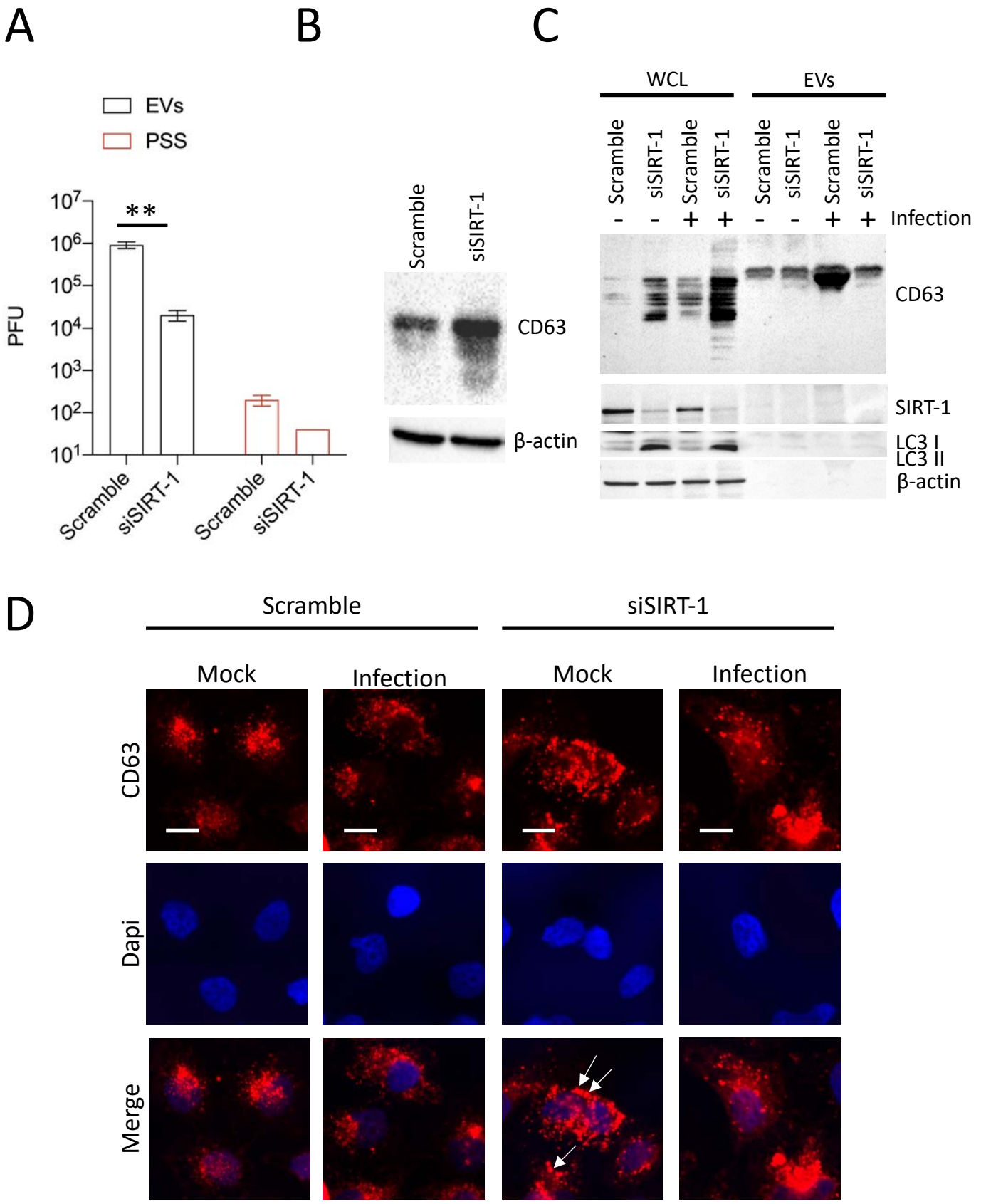

Fig. 3 SIRT-1 KD decreases EV-D68 extracellular titers in ATG-7 KO cells

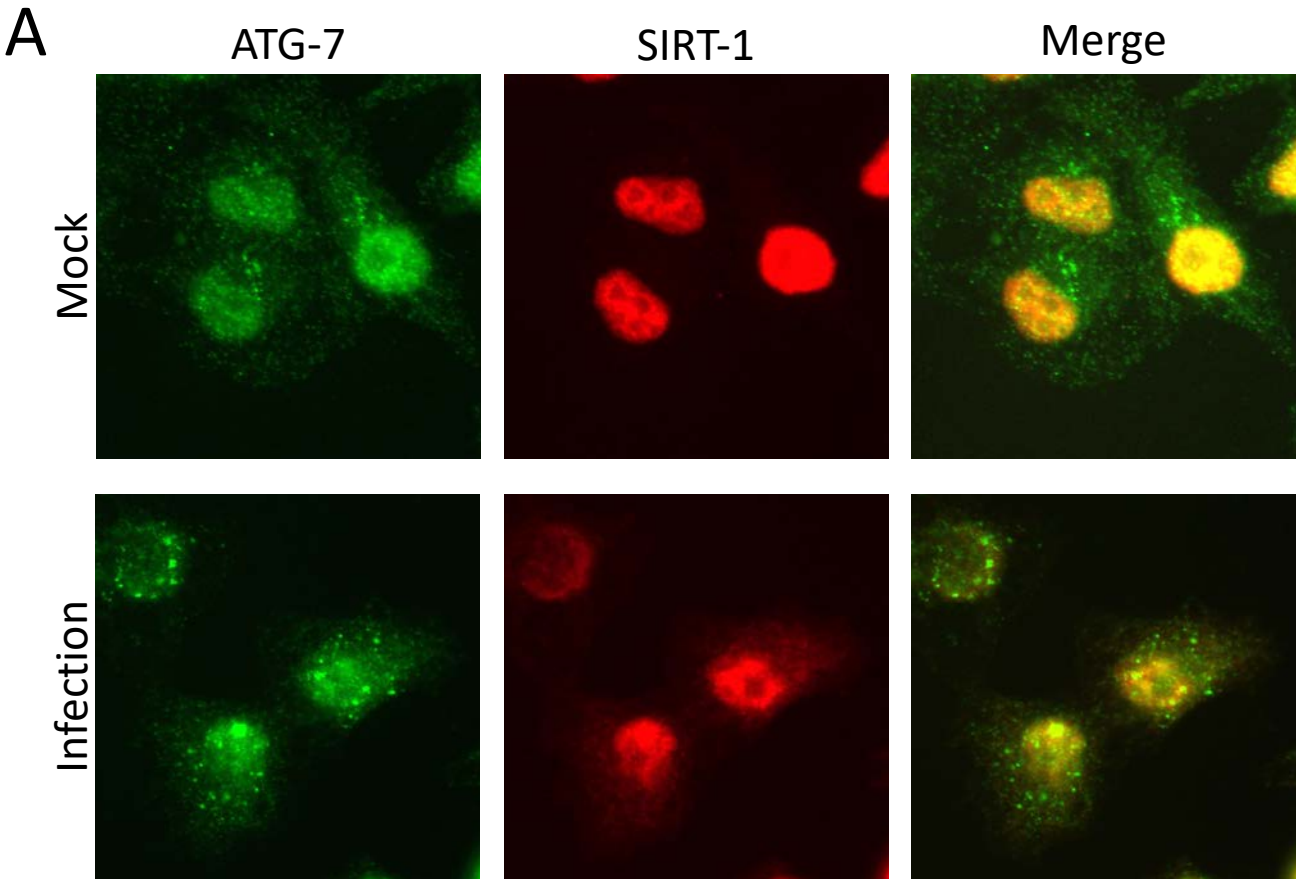

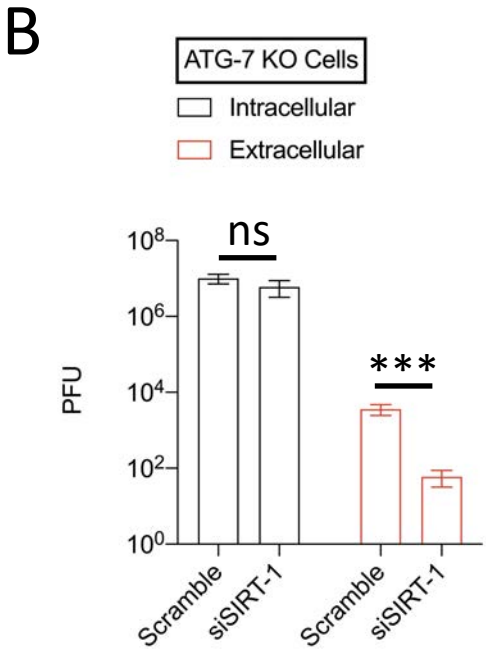

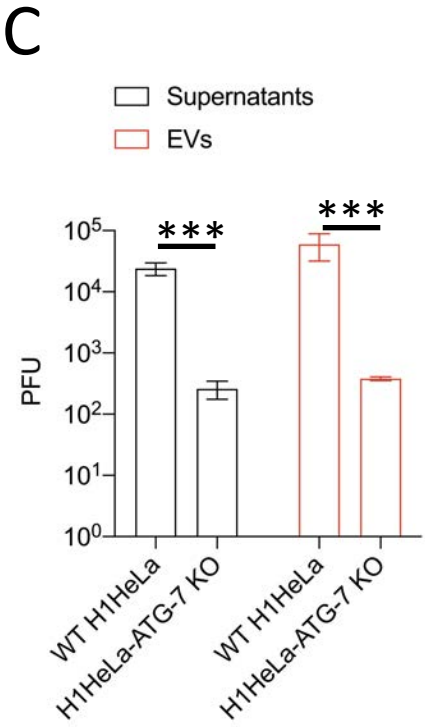

Fig. 4 EV-D68 infection changes SIRT-1's subcellular localization

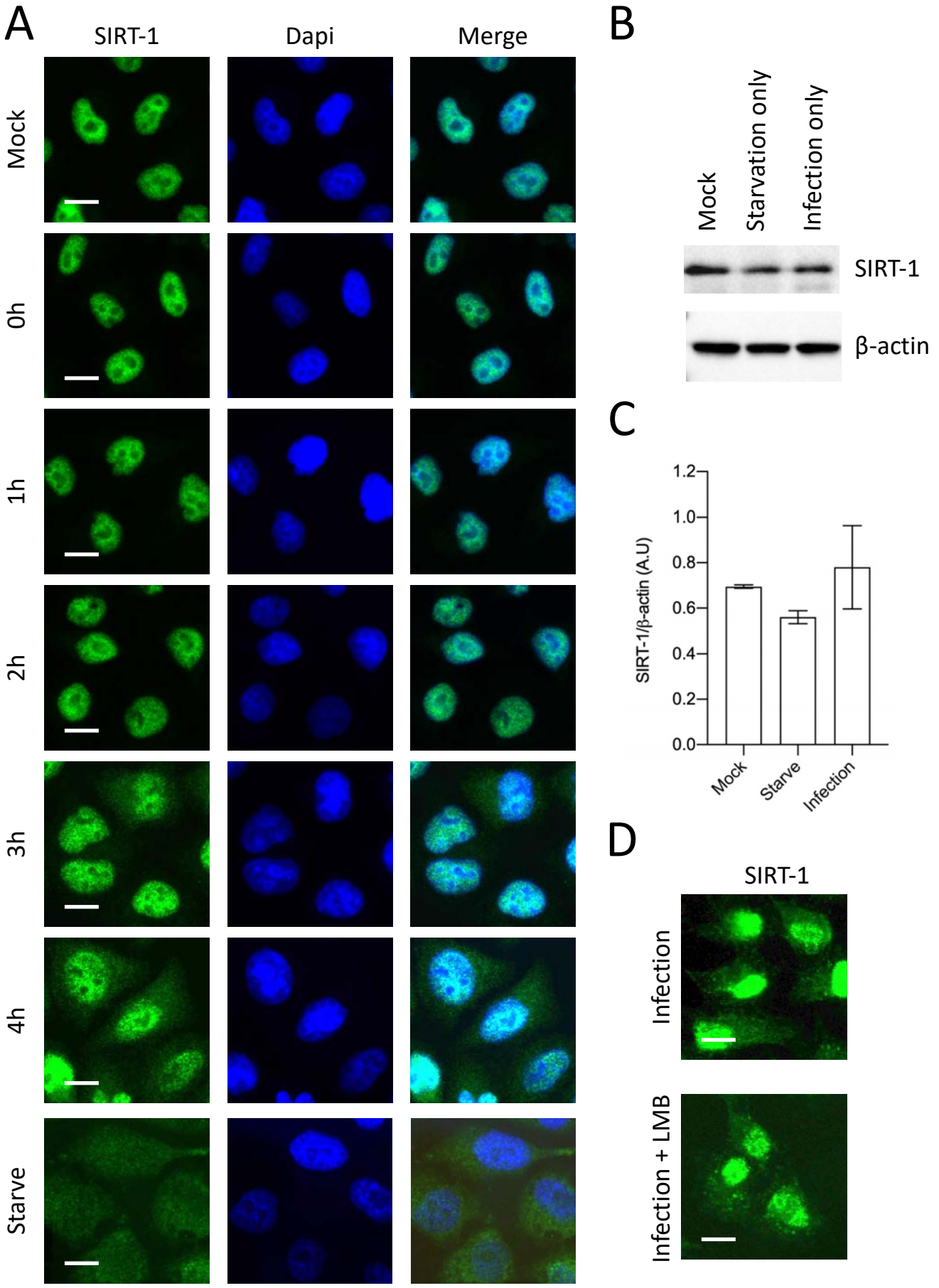

Fig. 5 SIRT-1 is not required EV-D68 entry and RNA replication

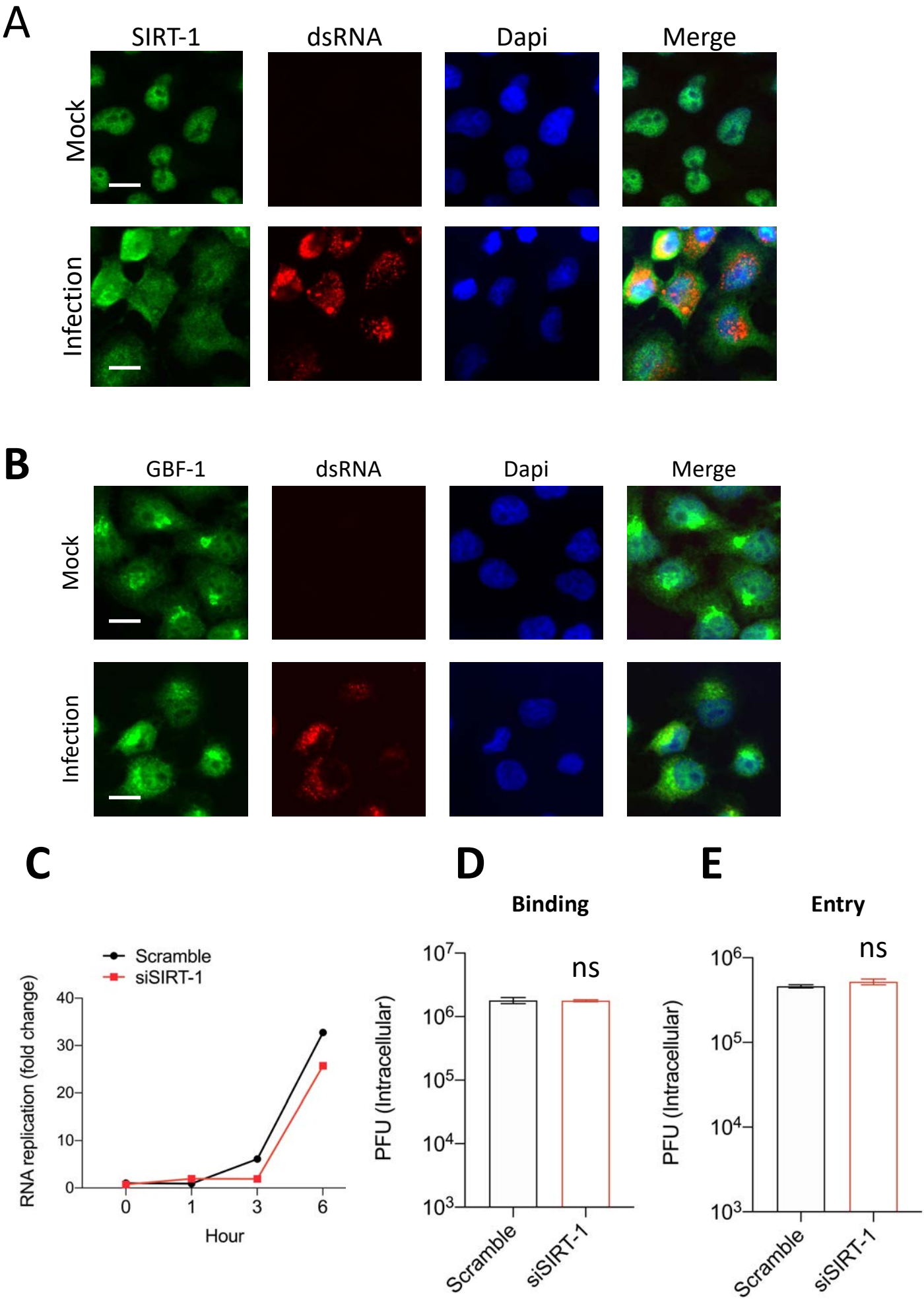

Fig. 6 PV, not CVB3, induces SIRT-1 translocation to the cytosol

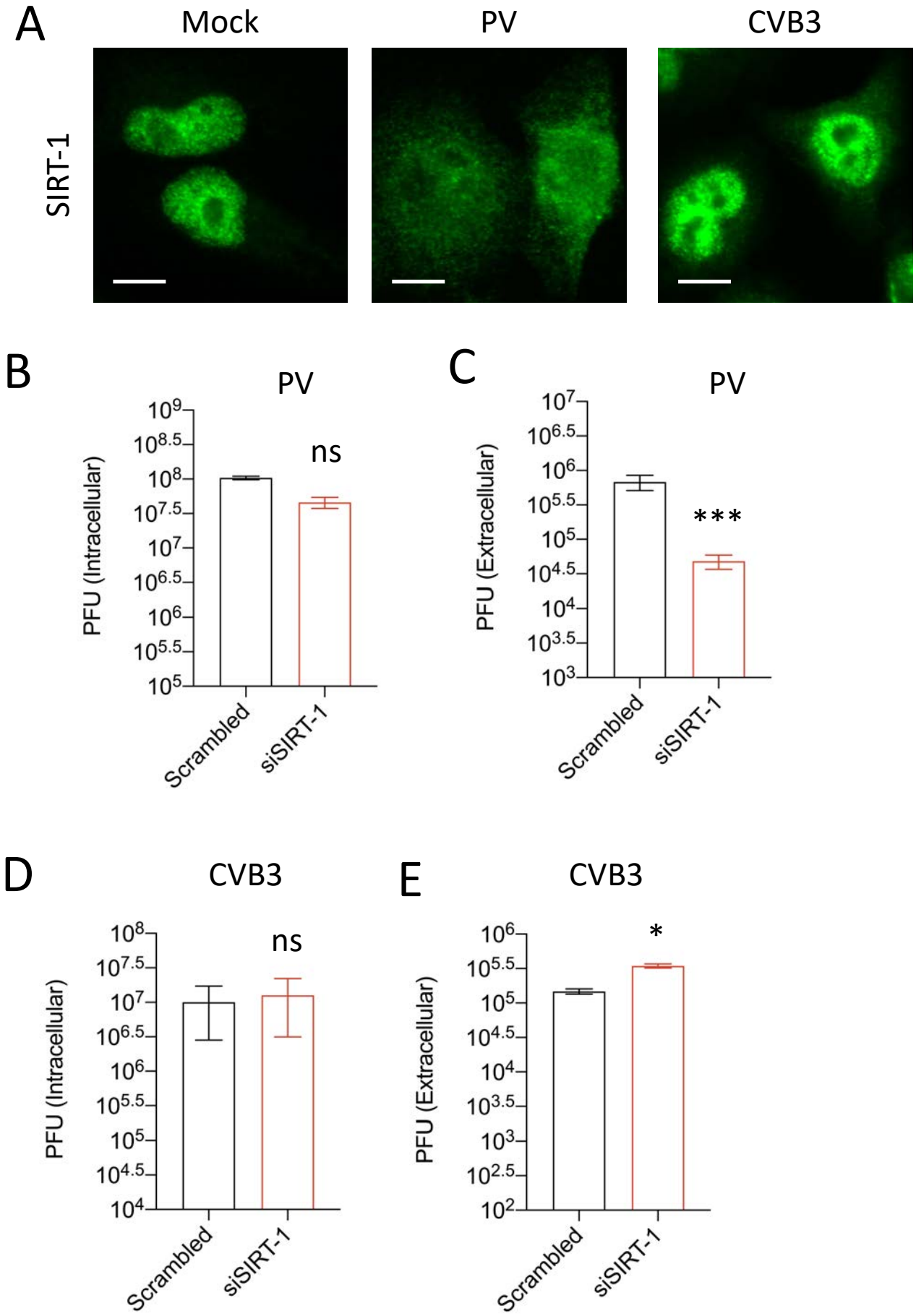

Fig. 7: SARS-CoV-2 induces SIRT-1 translocation to the cytosol

A

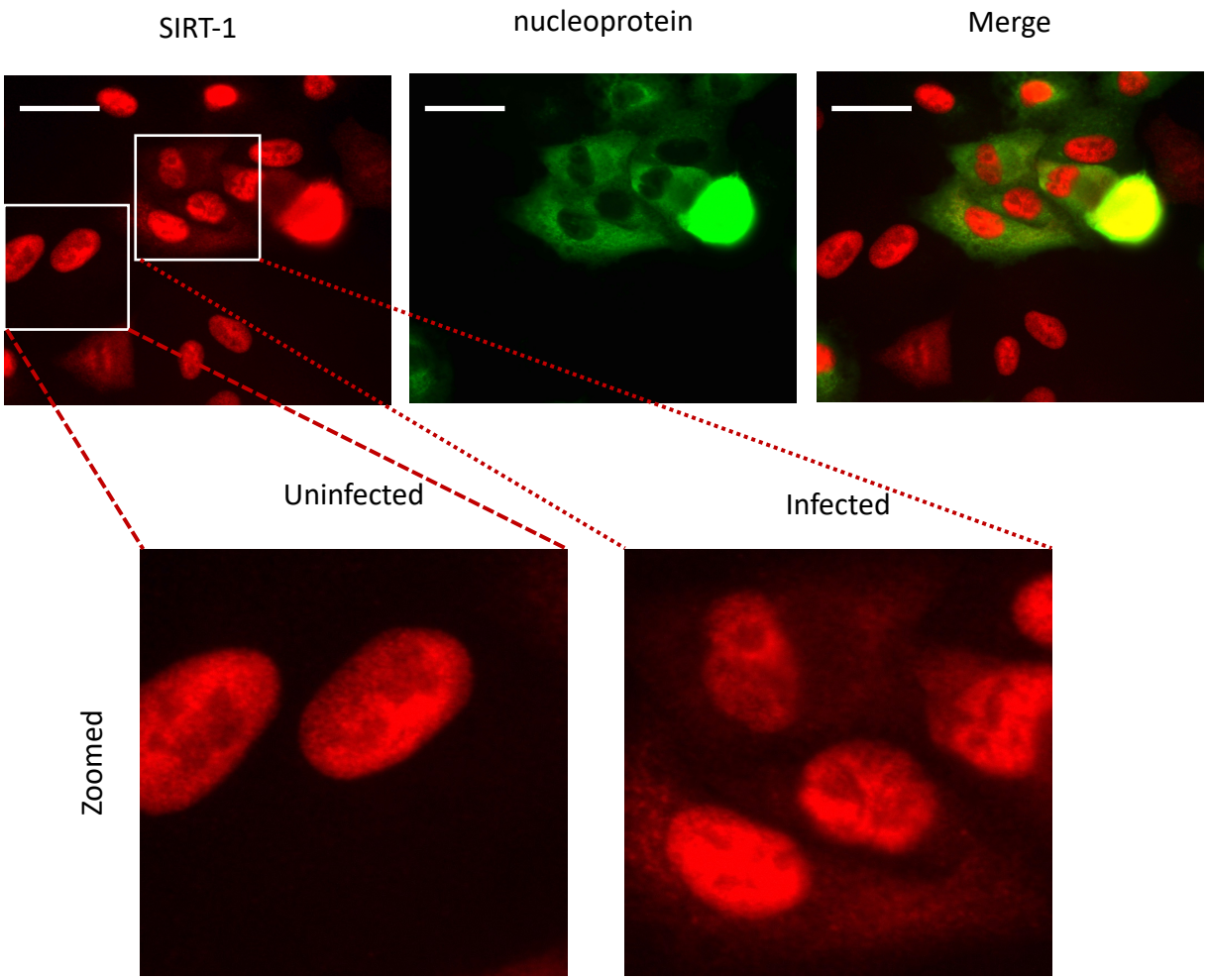

B

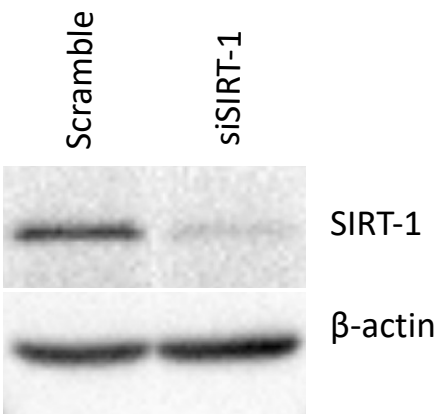
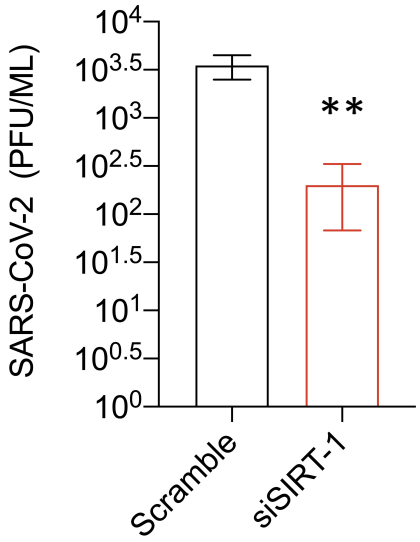
C